Conformational Analysis of Seven-Membered Ring Chelates, 1

Conformations and Dynamic Behaviour of Rhodium Complexes with 1,4-Bis(diphenylphosphanyl)butane, DIOP and Its HO Analogue

Renat Kadyrov,*[a] Armin Börner,[a] and Rüdiger Selke[a]

Keywords: Conformation analysis / Molecular modelling / NMR spectroscopy / Seven-membered chelates / Rhodium / Ab initio calculations

The temperature dependence of NMR spectra of $[(L)Rh(cod)]BF_4$ complexes with L = dppb (**1**), (*R*,*R*)-diop (**2**) and (*R*,*R*)-HO-diop (**3**) has been examined. Molecular mechanics and ab initio calculations on the [{1,4-bis(dimethylphosphanyl)butane}Rh^+(diolefin)] complex predict local energy minima for all twist-chair (TC_1, TC_2 = TC_7, TC_3 = TC_6, TC_4 = TC_5) and two boat (B_3 = B_6 and TB_1) conformations. Furthermore, ab initio calculations at the B3LYP/6-31G(d)/LANL2DZ level show that two minima are located in the wide-open region between the TC_7 and C_4 conformations. Relative B3LYP/6-31G(d) energies of the B_3, TC_1 and {C_4-TC_7} conformations are 0.0, 0.71 and 0.97–1.08 kcal mol^{-1}, respectively. Analysis of crystallographic data contained in the Cambridge Structural Database shows that the majority of structures are concentrated in the region {C_4-TC_7} and close to B_3. The symmetrical doublet in the ^{31}P-NMR spectra is assigned to the fast equilibrium {TC_7-C_4} ⇌ TC_1 ⇌ {C_5-TC_2}. The resonances of the other species are consistent with B_3 = B_6 geometry. A fused dioxolane ring forces the chelate in diop complexes to adopt the B_4 = B_5 conformation. For both types of ligand the chair-like conformation is enthalpically preferred at low temperatures ($\Delta H°$ = 0.45–0.46 kcal mol^{-1}), whereas the boat-shaped structure predominates at temperatures above 200 K ($\Delta S°$ = 0.9–1.3 cal K^{-1} mol^{-1}). Line-shape analysis provides a boat pseudorotation barrier for complex **1** of $\Delta G^{\neq}$ = 5.9 kcal mol^{-1} and for **2** $\Delta G^{\neq}$ = 5.3 kcal mol^{-1} at 184 K. The free energy of activation at this temperature for the boat–chair interconversion is $\Delta G^{\neq}$ = 8.6 kcal mol^{-1} for complex **1** and $\Delta G^{\neq}$ = 8.0 kcal mol^{-1} for complex **2**.

Introduction

Chelating bis(phosphane) ligands play a dominant role in metal-catalyzed stereoselective syntheses.[1] The relationship between catalyst conformation and the product configuration is well established. In general, the observed asymmetric induction is attributed to discriminatory interactions between substrate and bulky phosphane substituents adjusted by the chiral conformation of the chelate.[2] In particular, asymmetric hydrogenation catalyzed by cationic rhodium complexes containing chiral phenyl-substituted five-membered bis(phosphane) chelates is one of the most intensively investigated stereoselective reactions. The generally accepted basis for the enantioselectivity is the concept of pseudo axial−equatorial arrangement of the *P*-phenyl groups based on the "edge-to-face" model.[3] The configuration of the hydrogenation product is determined by the δ or the λ conformation of the five-membered ring.[4]

Complexes based on seven-membered bis(phosphane) chelates hydrogenate with higher reaction rates. The enhanced catalytic activity is associated with the high degree of conformational flexibility of the chelate ring. Only very few solution-NMR studies on seven-membered chelate conformations have been performed.[5] Although the crystallographic data show that these chelates may adopt some non-symmetrical conformations,[6] recent NMR results have been interpreted in terms of C_2-symmetrical geometries.[5a,7] Accordingly, idealized C_2-symmetrical twist-chair and twist-boat conformations were involved in mechanistic considerations on the origin of the stereoselectivity.[4b,8]

We examined the conformations and dynamic behaviour of seven-membered chelate rings of three complexes $[(L)Rh(cod]BF_4$ with L = 1,4-bis(diphenylphosphanyl)butane (**1**), (*R*,*R*)-diop (**2**) and (*R*,*R*)-HO-diop (**3**); cod = 1,5-*cis*-cyclooctadiene (Scheme 1).

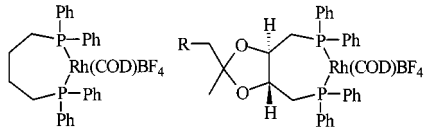

1 (dppb) **2** R = H (diop) **3** R = OH (HO-diop)

Scheme 1

First, we calculated all basic conformations of the chelate ring by applying a simple MMX force field. The results of these calculations were used as input for ab initio calculations at the B3LYP/6-31G(d)/LANL2DZ level. X-ray data available from the Cambridge Structural Database were analyzed to verify the predicted favoured conformers. Low-temperature NMR spectroscopy was used to obtain infor-

[a] Institut für Organische Katalyseforschung an der Universität Rostock e.V.
Buchbinderstraße 5−6, D-18055 Rostock, Germany
Fax: (internat.) + 49(0)381/4669324
E-mail: renat.kadyrov@ifok.uni-rostock.de

  1434−1948/99/0404−0705 $ 17.50+.50/0

mation about the conformers present in solution and their dynamic properties.

Results

Conformations of the Seven-Membered Chelate Rings — Computed versus Experimental Structures

Molecular mechanics calculations have been used to establish the main conformational features of cycloheptane and some seven-membered heterocycles.[9] Calculations based on empirically determined potential functions were also successfully applied to the solution of structural problems of the coordination chemistry[10] especially of square-planar transition-metal complexes.[11] Recently, some reports demonstrated the utility of the molecular modeling program PCMODEL for determining minimum-energy structures of a variety of flexible complexes.[12] For the following discussion we use the notation for conformations introduced by Hendrickson,[13] labelling the position of the metal as 1.

In order to reduce the independently varied parameters, we have involved the corresponding dimethylphosphanyl derivative in the calculations. The structure of [{1,4-bis(dimethylphosphanyl)butane}Rh^+(cod)] = [(dmpb) Rh^+(cod)] was constructed by use of PCMODEL 4.0 with the parameter set and interactions described in the Experimental Section. At first, we carried out a series of calculations to search all relative low-energy local minima. For identification the conformations were analyzed in terms of ring-puckering coordinates. These coordinates (q_2, q_3, ϕ, ψ) were calculated from the Cartesian coordinates according to the original Cremer−Pople method.[14] The puckering amplitudes q_i were replaced by the total puckering amplitude Q and the angle θ:

$$q_2 = Q \cos \theta$$
$$q_3 = Q \sin \theta$$

The angle θ specifies the relative contribution of boat- and chair-like conformations. The chair-twist-chair family has for cycloheptane a θ value of about 66°. Boat-twist-boat conformers are characterized by $\theta \approx 0°$.[15] The minimization procedures gave four different twist-chair conformations (TC_1, $TC_7 = TC_2$*, $TC_6 = TC_3$*, $TC_5 = TC_4$*) and two boat forms (TB_1 and distorted $B_3 = B_6$*), where $TC_7 = TC_2$* means that TC_2 is enantiomeric to TC_7. The calculated energies and geometries of conformers are summarized in Table 1. The twist-chair conformations are connected by a pseudorotation pathway as are the twist-boat conformations. Figures 1 and 2 display the energy profiles in the course of pseudorotation. The calculation of the energy variation along the pseudorotation pathways is detailed in the Appendix.

The geometries determined using MMX force fields for these conformers were used as starting points for the ab initio calculations of the [(dmpb) $Rh^+(C_2H_4)_2$]. For all six conformers, full geometry optimizations were done at the B3LYP/6-31G(d)/LANL2DZ level. The calculated energies and geometries of conformers are given in Table 1. These calculations also indicate the B_3 structure to be of lowest energy with the TC_1 structure only 0.71 kcal mol^{-1} higher in energy. Since the pseudorotation $TC_7 \rightleftharpoons C_4 \rightleftharpoons TC_1$ changes mainly the P−Rh torsion angle (see Appendix), it is expected that the behaviour of the potential energy curve in this region is affected by electronic interactions of the phosphane moiety with the metal centre. Therefore, we examined the potential energy surface along the TC_7 to TC_1 pseudorotation at the B3LYP/6-31G(d) level. At first, partial geometry optimization was performed for C_4 (at ϕ = 50°) conformation with fixed cyclic Rh−P torsion angle. Full optimization, in the next step, led to the additional minimum at ϕ = 30° (distorted C_4). Furthermore, the spline interpolation gave a nearly flat potential-energy curve for the $TC_7 \rightleftharpoons C_4 \rightleftharpoons TC_1 \rightleftharpoons C_5 \rightleftharpoons TC_2$ pseudorotation.

Table 1. Puckering coordinates[a] of optimized molecular geometries and calculated relative energies[b] for [(dmpb)Rh^+(cod)] at the MMX level and for [(dmpb) $Rh^+(C_2H_4)_2$] at the B3LYP/6-31G(d)/LANL2DZ level

Conformation	Method	Q	θ	ϕ	ψ	ΔE
Distorted B_3	MMX	1.51	9.1	29.1	10.5	0
	B3LYP	1.47	8.6	30.1	9.5	0
TB_1	MMX	1.15	11.1	90	90	5.69
	B3LYP	1.17	4.1	90	90	6.38
TC_7	MMX	1.19	49.5	13.2	49.2	2.22
	B3LYP	1.12	48.4	12.4	50.9	1.08
TC_1	MMX	0.97	53.5	90	90	2.27
	B3LYP	0.88	56.1	90	90	0.71
Distorted C_4	B3LYP	1.02	52.3	29.9	60.3	0.97
TC_6	MMX	1.08	38.9	−64.9	37.3	3.22
	B3LYP	1.21	45.5	-49.5	27.8	3.44
TC_5	MMX	1.03	43.2	-134.1	7.4	3.50
	B3LYP	1.00	31.5	-142.0	8.8	1.85

[a] Q in Å and θ, ϕ, ψ in°. − [b] In kcal mol^{-1}.

MMX and B3LYP calculations indicate that the most stable conformer is boat-shaped, and is represented in the energy hypersurface by a large well between canonical B_3 and TB_4 geometries. For clarity, we define this conformer as distorted B_3. The C_2-symmetrical TB_1 form, mostly mentioned in the literature, is 6.4 kcal mol^{-1} above. Pseudorotation $B_3 \rightleftharpoons B_6$ proceeds via B_1 and requires, according to the MMX molecular mechanics model, an activation energy of 5.5 kcal mol^{-1}. In the next family three low-energy chair forms, TC_7, distorted C_4 and TC_1, are separated by very low barriers. The barrier to the succeeding TC_6 at the molecular mechanics level is not as high as 3 kcal mol^{-1}, whereas TC_6 and TC_5 are separated by a barrier of approximately 7 kcal mol^{-1}. Therefore, conformation $TC_5 = TC_4$ should be distinguishable in the low-temperature NMR spectra from the fast equilibrium $TC_6 \rightleftharpoons TC_7 \rightleftharpoons TC_1 \rightleftharpoons TC_2 \rightleftharpoons TC_3$. Note that barrier calculations using the MMX model reflect exclusively steric and electrostatic influences of the inorganic unit of the molecule and give large deviations from those calculated by ab initio methods if substantial electronic interactions with the metal centre come into play.

We have analyzed the conformational preferences of the seven-membered chelate rings with 1,4-diphosphanylbutane fragments using crystallographic data collected in the Cambridge Structural Database (CSD).[16] There are 51 structures containing M(dpb) and M(diop) fragments, where M = transition metal of group VI−VIII and dpb = 1,4-diphosphanylbutane. Crystallographic data for these structures were saved in FDAT format and then the Cartesian coordinates of the chelating seven-membered ring were extracted. Puckering coordinates (Q, θ, ϕ, ψ) were calculated according to the procedure outlined above. 37 unique fragments present in the crystal structures are characterized by θ = 45−67° and can be identified as chair-like structures. Figure 1b displays scatter plots of phase angles ϕ, ψ for these fragments and projections of a pseudorotation map for the chair-twist-chair forms of cycloheptane. The majority of structures are concentrated in the region between two neighbouring cycloheptane conformations {C_4-TC_7} and only one of them exists in the TC_1 conformation.[28] The most obvious consequence is that the preferred chair-like conformation of the metal chelates with a diphosphanylbutane fragment located between the C_4 and TC_7 forms. Evidently, the shape of this conformation depends on the metal and nature of the co-ligands. Several structures were found in TC_5 and TC_6 conformations indicating the stabilization of these conformations in accordance with the theoretical calculations.

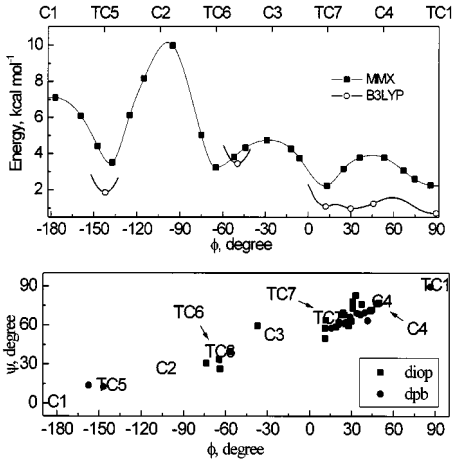

Figure 1. (a) (top) Relative MMX energy as a function of chair ⇌ twist-chair pseudorotation phase ϕ for [(dmpb)Rh^+(cod)] and relative energies of the B3LYP/6-31G(d)/LANL2DZ optimized geometries for [(dmpb) $Rh^+(C_2H_4)_2$]; (b) (bottom) scatter plot of pseudorotation phases ϕ, ψ for transition metal complexes bearing 1,4-diphosphanylbutane (●) or diop (■) fragments contained in CSD and projection of pseudorotation map for the chair ⇌ twist-chair forms of cycloheptane

The next 25 fragments are specified by θ = 3−11° and, therefore, may be assigned to the boat-like conformation. The structures on the scatter plot (Figure 2) are distributed in the regions of B_5−TB_6 conformations for the diop chelates and between B_3−TB_4 canonical forms for the chelates without rigid backbone. In this case, the calculations show satisfactory agreement with the structural information obtained by X-ray analysis. Since θ ≈ 0°, only ϕ defines the conformations in the boat family and the pseudorotation path is just a function of ϕ. Thus, one has to expect only one stable boat-shaped form for the seven-membered ring chelates, which can be represented as distorted B_3 for dpb. Although the twist-boat is more stable than the boat, introduction of the heteroatomic P−M−P fragments into the cycloheptane ring avoids some H/H bond eclipsing in the B_3 conformation. On the other hand, a large difference in the bond lengths forces the heterocyclic seven-membered ring out of its canonical boat and twist boat forms.

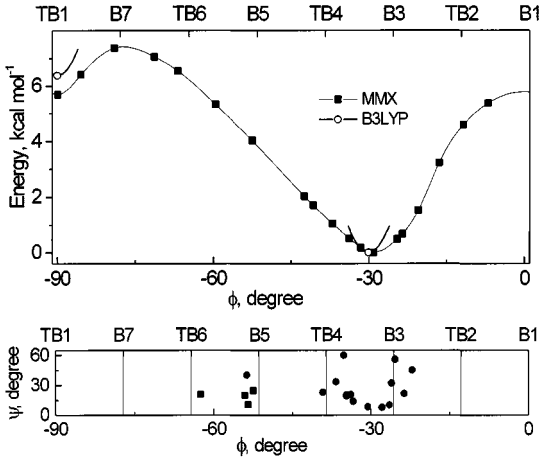

Figure 2. (a) (top) Relative MMX energy as a function of twist-boat ⇌ boat pseudorotation phase ϕ for [(dmpb)Rh^+(cod)] and relative energies of the B3LYP/6-31G(d)/LANL2DZ optimized geometries for [(dmpb) $Rh^+(C_2H_4)_2$]; (b) (bottom) scatter plot of pseudorotation phases ϕ, ψ for transition metal complexes bearing 1,4-diphosphanylbutane (●) , diop (■) fragments contained in CSD and projection of pseudorotation map for the twist-boat ⇌ boat forms of cycloheptane

Complexes bearing chiral diop-type ligands provide an interesting example of the *trans* fusion of a dioxolane ring to a seven-membered chelate ring. According to Hendrickson,[9a] *trans* fusion of cyclopentane to cycloheptane should be most favoured at either 2e-3e or 3e-4e of the twist chair that correspond to the 4e-5e-TC_6 and 4e-5e-TC_7 conformations in our definition. In fact, most structures examined by X-ray analysis reveal a 4e-5e-{C_4-TC_7} conformation and several structures were found in a 4e-5e-TC_6 conformation, as illustrated in Figure 1. The *trans* fusion across the 4−5 bond to the B_3 = B_6* conformation requires 4a-5e or 4e-5a orientation with a fusion angle of approximately 120° and, thus, would strain the system. On the contrary, the B_4 = B_5* conformation allows an energetically more favourable fusion at the 4e-5e position. This conformer is likely to be the most stable boat-shaped form of the diop chelates (Figure 2).

Variable-Temperature NMR Studies of Complexes

The Rh^I complexes with dppb (**1**), (*R*,*R*)-diop (**2**) and (*R*,*R*)-HO-diop (**3**) exhibit temperature-dependent NMR spectra. The sharp doublet in the $^{31}P\{^1H\}$-NMR spectrum of **2** in a mixture of $CHCl_2F/CD_2Cl_2$ (3:1) at 250 K (Figure 3) undergoes coalescence at approximately 188 K as the

sample is cooled. Two doublets separate below 179 K in a 1:0.45 intensity ratio, similar to those briefly described by Brown and Chaloner.[7]

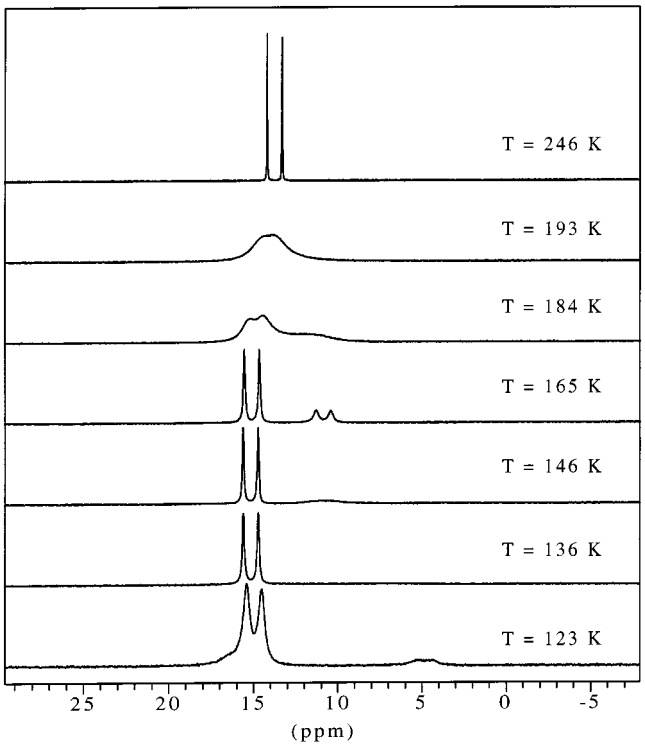

Figure 3. Variable-temperature $^{31}P\{^1H\}$-NMR spectra of complex **2** in $CD_2Cl_2/CHFCl_2$

While the downfield doublet at a chemical shift of δ = 14.7 due to the major isomer **A** sharpens as the temperature is lowered further, the upfield signals at δ = 10.5 of isomer **B** broaden and then separate below 123 K into two broad signals with Rh coupling at $\delta \approx 5.2$ and 15.9. The variable-temperature spectra of the complexes **1** and **3** show the same behaviour as for **2**, if one takes into account that the phosphorus atoms in **3** are diastereotopically not equivalent. The low-temperature ^{31}P-NMR data are included in Table 2. It is noteworthy that the resonances of the major species **A** in complex **1** are shifted to lower field compared to that in **2** and **3**. However, those of the minor species **B** in complex **1** exhibit significantly larger differences in chemical shifts than those in compounds **2** and **3**.

Structural Assignment of the Exchanging Sites in Solution

Detailed variable-temperature NMR studies of [(diop-4NMe$_2$)PtCl$_2$] confirmed that the species characterized at low temperature by a downfield phosphorus resonance has a rigid conformation with C_2 symmetry.[5a] The upfield signal broadens significantly as the temperature is lowered further. This indicates the flexibility of this species and that the C_2 symmetry is time-averaged.[5a] These results are in accordance with our observations of ^{31}P-NMR spectra of complexes **2** and **3**. Inspection of the X-ray data for [(HO-diop)Rh(cod)]BF$_4$ reveals two conformations for the seven-membered chelate in the solid state.[17] One of the ring conformations can be described as C_4 chair and the other as distorted B_5 boat (Figure 4).

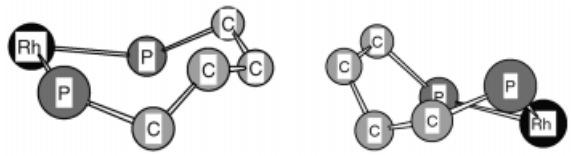

Figure 4. View of two chelate ring conformations as present in crystalline complex **3**: C_4 (left) and distorted B_5 (right)

Therefore, we assign the AMX pattern of the isomer **B** in the spectra of **2** and **3** at 123 K to the dissymmetric distorted B_5 structure which undergoes pseudorotation with an appreciable barrier to give a symmetrized doublet above 155 K. Note that the pseudorotation segment $C_5 \rightleftharpoons TC_1 \rightleftharpoons C_4$ connects two enantiomeric chair forms. According to the consideration in the first section this pseudorotation should be almost completely free. The symmetrical doublet at δ = 15 of the isomer **A** may be assigned to this fast equilibrium, because two phosphorus atoms remain equivalent just at very low temperatures. The dynamic phenomenon observed in the ^{31}P-NMR spectra between 210 K and 180 K is caused by the interconversion of two families of conformations. These assignments are consistent with recent solution-NMR investigations of similar compounds.[5a]

By analogy, it appears reasonable to assign the twist-chair conformation to the species **A** in the conformational equilibrium of the complex without a rigid backbone. The low-field shift of the **A** resonances in the case of complex **1** in comparison with those of complexes **2** and **3** is caused by other twist-chair conformations being appreciably popu-

Table 2. $^{31}P\{^1H\}$-NMR data of the complexes in $CD_2Cl_2/CHFCl_2$[a,b]

Complex	T [K]	P(**A**)	P_1(**B**)	P_2(**B**)
1	246		25.18 (J_{RhP} = 143.2)	
	124	27.84 (J_{RhP} = 141.6)	7.77 (J_{RhP} = 138)	39.57 (J_{RhP} = 146)
2	246		13.08 (J_{RhP} = 143.9)	
	126	14.95 (J_{RhP} = 143.8)	4.82 (J_{RhP} = 142)	16.37 (J_{RhP} = 142)
3	246		12.57 (J_{RhP} = 143.95)	
	135	14.17 (J_{RhP} = 143.0) 14.69 (J_{RhP} = 142.9) (J_{PP} = 39.0)	ca. 4−6	ca. 15−16

[a] Chemical shifts relative to H_3PO_4, coupling constants in Hz. − [b] J_{PP} could not be derived from the broad lines in the spectra.

lated in the fast conformational equilibrium. According to X-ray data the chelate ring in complex **1** has a B_3-shaped structure in the solid state.[18] Based on these data we assign the B_3-like conformer to the species **B** in solution. Evidently, this B_3-shaped moiety exhibits a much larger difference in chemical shifts than the B_5-like geometry.

Thermodynamic and Kinetic of Exchange

The equilibrium constants $K = [\mathbf{B}]/[\mathbf{A}]$ for the $\mathbf{A} \rightleftharpoons \mathbf{B}$ interconversion for the complexes **1** and **2** have been calculated at different temperatures by ^{31}P-NMR integration. The evaluated energy differences $\Delta G^\circ = -RT \ln K$ have been plotted against T giving a satisfactory linear least-squares fit (Figure 5). Linear-regression analysis of these data allows calculation of the enthalpy and entropy values which are shown in Table 3. The obtained values for ΔS° suggest that the boat-shaped conformation has a substantially higher entropy than the chair-like and is predominant at higher temperatures.

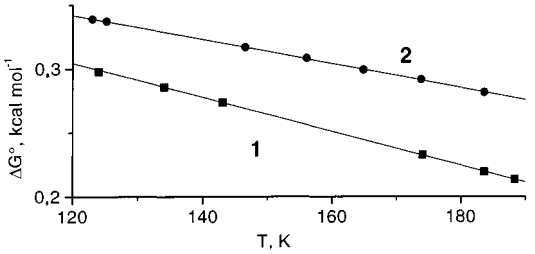

Figure 5. Plots of ΔG° vs. temperature obtained by $^{31}P\{^1H\}$-NMR integration for complexes **1** (■) and **2** (●)

Table 3. Thermodynamic and kinetic data for the complexes[a,b]

Complex	**1**	**2**
ΔG°_{AB}	0.22	0.28
ΔH°_{AB}	0.45 ± 0.02	0.46 ± 0.02
ΔS°_{AB}	1.3	0.9
$\Delta G^{\neq}_{AB}$	8.6	8.0
$\Delta H^{\neq}_{AB}$	8.4 ± 0.1	7.6 ± 0.2
$\Delta S^{\neq}_{AB}$	1.5 ± 1	3 ± 1
$\Delta G^{\neq}_{BB'}$	5.9	5.3
$\Delta H^{\neq}_{BB'}$	6.0 ± 0.1	5.9 ± 0.1
$\Delta S^{\neq}_{BB'}$	−1 ± 1	−3 ± 1

[a] ΔG and ΔH in kcal mol^{-1}, ΔS in cal mol^{-1} K^{-1}. – [b] All ΔG are given at 184 K.

By application of WIN-DYNAMICS,[19] spectra were simulated and iteratively fitted to the experimental spectra in order to evaluate the rate constants at various temperatures. The line-shape analysis was performed on the basis of the three-site exchange model (Scheme 2).

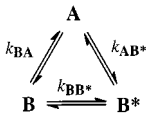

Scheme 2. Three-site exchange

The resulting rate constants as a function of the temperature were used to construct an Eyring plot (Figure 6). The activation parameters obtained from linear regression analysis are given in Table 3. The activation entropies are close to zero. The values of activation energy $\Delta G^{\neq}$ for complex **2** are lower than those found for complex **1**.

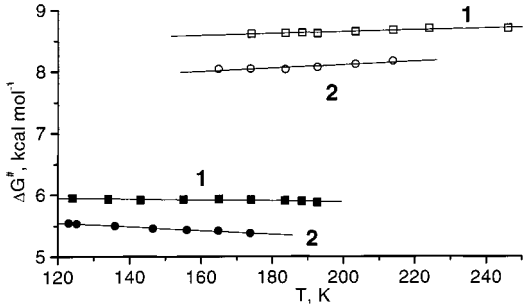

Figure 6. Eyring plots of $\Delta G^{\neq}$ vs. temperature from the kinetic data for compexes **1** (□, ■) and **2** (○, ●); the open symbols are the data for the $\mathbf{B} \rightleftharpoons \mathbf{A}$ exchange and the closed ones for the $\mathbf{B} \rightleftharpoons \mathbf{B}$ exchange

Discussion

NMR investigations by Brown and Chaloner[7] show the conformational flexibility of the seven-membered diop chelate ring. A dynamic equilibrium between at least two different basic conformers was manifested. Activation energies between 9.6 to 11.7 kcal mol^{-1} were obtained for Pt, Pd and Ni complexes at 220−250 K.[7][20] We have found activation energy values $\Delta G^{\neq}$ of the boat-to-chair interconversion of 8.6 kcal mol^{-1} in complex **1** and 8.0 kcal mol^{-1} in **2** at 184 K. These values are comparable with the barrier for chair-to-boat interconversion of about 8.5 kcal mol^{-1} in cycloheptane.[9c,21] The lower inversion barrier in the diop complex is in accordance with the diminished cyclohexane interconversion barrier by fusion with a cycloheptane ring and reflects increasing strain energy in the ground state.[22]

Nevertheless, the experimentally observed C_2 symmetry of the chair conformation is apparently time-averaged. The ab initio calculations show that part of a family of flexible conformers $TC_7 \rightleftharpoons C_4 \rightleftharpoons TC_1 \rightleftharpoons C_5 \rightleftharpoons TC_2$ form a large potential well with minima separated by very low barriers. This explains why X-ray studies show in most cases an unsymmetrical C_4 or TC_7 conformation,[6] but low-temperature NMR studies reveal C_2-symmetrical species. The pseudorotation in the boat family proceeds with higher activation energy. The observed barriers are 5.9 kcal mol^{-1} for **1** and 5.3 kcal mol^{-1} for **2**. These are much higher than calculated for cycloheptane (0.5 kcal mol^{-1}),[15] but are in surprisingly good accordance with that calculated using a simple MMX model for [(dmpb)Rh$^+$(cod)] (5.5 kcal mol^{-1}). Note that for diop-type chelates pseudorotation $B_4 \rightleftharpoons B_5$ proceeds via TB_1.

In fact, entropy favours the boat form, whereas the chair-like conformation is enthalpically stabilized and predominates at 124 K by only $\Delta G^\circ = 0.30$ kcal mol^{-1} in complex **1** and by $\Delta G^\circ = 0.34$ kcal mol^{-1} in **2**. Because of the coun-

tertrend of $\Delta H°$ and $\Delta S°$ there is a cross-over of the equilibrium constant K = [**B**]/[**A**] at about 180−200 K. Above that temperature the boat conformation is more stable. The relatively large magnitude of the entropy difference $\Delta S°$ = 0.9−1.3 cal K^{-1} mol^{-1} comes as somewhat of a surprise. On the other hand, the error in the $\Delta S°$ determination consists of the inaccuracy in temperature determination and the error of integration of the broadened lines in the NMR spectra at low temperatures. We could not ascertain the exact source of the error. Thus, the given values of ΔS should be taken with care.

We can conclude that seven-membered diphosphane chelates exist in two conformations, chair- and boat-like, with the position of equilibrium depending on the temperature. The $\{TC_2\text{-}C_5\}$ = $\{TC_7\text{-}C_4\}$ structure represents the enthalpically most stable conformation and undergoes pseudorotation readily. The other conformer has the distorted B_3 = B_6 geometry for dppb and distorted B_4 = B_5 arrangement for diop chelates. This moiety undergoes a conformational inversion with a higher barrier.

Experimental Section

General Remarks: All solvents were freeze-pump-thaw-degassed using a vacuum line and stored under argon. The diolefin complexes [(dppb)Rh(cod)]BF_4 and [(diop)Rh(cod)]BF_4 were prepared by standard methods from ligand and [(acac)Rh(cod)] by treatment with HBF_4.[23] The preparation of [(HO-diop)Rh(cod)]BF_4 has been previously described.[24] The NMR samples were prepared under an inert gas and the solvents were transferred under vacuum. The solution was degassed with one freeze-pump-thaw cycle and then the tube was sealed. − The NMR spectra were recorded with a Bruker ARX400 spectrometer. The ^{31}P chemical shifts are reported in δ units relative to H_3PO_4. The temperature of the NMR probe was calibrated using a methanol temperature standard and the low-temperature range by extrapolation of the difference in chemical shifts of CHF_2OH in ^1H-NMR spectra.

Molecular Mechanics Calculations: Except where noted, the molecular mechanics parameters were set to the PCMODEL[25] default values. The force field about the metal ion was designed so that the metal−ligand distances and the ligating atom−ligating atom interactions determined the shape of the coordination sphere. Default bending force constant for ideal P−Rh−P angle of 90° in a square-planar geometry was used. All other metal-dependent interactions were treated exactly as in a points-on-a-sphere approach.[26] This was accomplished by setting the L−Rh−L angle parameters, and L−Rh−L−A and Rh−L−A−B torsional parameters to zero.

Ab Initio Calculations: All calculations were performed using the B3LYP hybrid functional. The full geometry optimizations have been carried out with LANL2DZ basis for rhodium, associated with the relativistic effective core potential, and the 6-31G(d) basis set for all other atoms. The calculations were performed with the program GAUSSIAN 94.[27]

Appendix: To calculate the energy along a pseudorotation path note that the sequence $TC_i \rightarrow C_{i-3} \rightarrow TC_{i+1}$ represents the elementary steps in the chair pseudorotation. Moreover, bond dihedral angles ω_i in one TC_i conformation change sign going on to the next TC_{i+1} conformation in the pseudorotation sequence as shown in Scheme 3.

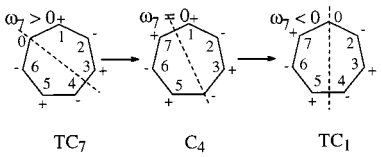

Scheme 3. Sequence of the elementary steps in the chair pseudorotation

In addition, signs of the out-of-plane displacements (z coordinates) of each cyclic atom are drawn here for visual representation of conformation. The sequence $TB_i \rightarrow B_{i+1} \rightarrow TB_{i+2}$ constructs a pseudorotation in a boat family (Scheme 4).

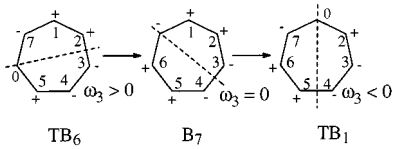

Scheme 4. Sequence of the elementary steps in the boat pseudorotation

Therefore, each intermediate form between two twisted forms is unequivocally defined by a corresponding torsional angle. That is ω_i for the $TC_i \rightarrow TC_{i+1}$ movement and ω_{i+4} for the $TB_i \rightarrow TB_{i+2}$ conversion. Starting at the value of the initial twisted form the magnitude of ω was incremented (decremented) in 5° or 10° steps until the next twisted conformation was reached and the conformation of minimum energy was found for each given value of ω. The Cartesian coordinates of the optimized (by keeping ω constant) geometries were transformed into the puckering coordinates. The energies thus obtained for each value of ω were plotted against a phase angle ϕ and connected by an interpolation curve to give cuts of the energy surface along the pseudorotation tracks between two of each twisted forms. These cuts were combined in common plots for chair and boat pseudorotations, as shown in Figures 1 and 2.

Acknowledgments

The authors thank the Max-Planck-Gesellschaft, the BMBF (Förderkennzeichen 03D0053C5) and the Fonds der Chemischen Industrie for financial support, Dr. Shigehiro Yamaguchi for providing X-ray structure data and Dr. G. Stark for helpful discussions.

[1] H. Brunner, W. Zettlmeier *Handbook of Enantioselective Catalysis with Transition Metal Compounds*, vol. 2, Ligands − References, VCH Verlagsgesellschaft, Weinheim, **1993**, p. 359.

[2] [2a] M. D. Fryzuk, B. Bosnich, *J. Am. Chem. Soc*. **1978**, *100*, 5491−5494. − [2b] D. A. Slack, I. Greveling, M. C. Baird, *Inorg. Chem.* **1979**, *18*, 3125−3132. − [2c] P. A. MacNail, N. K. Roberts, B. Bosnich, *J. Am. Chem. Soc*. **1981**, *103*, 2273−2280. − [2d] B. Bosnich, N. K. Roberts *Adv. Chem. Ser.* **1982**, *196*, 337−354. − [2e] J. Bacos, I. Toth, B. Heil, G. Szalontai, L. Parkanyi, V. Fülöp, *J. Organomet. Chem.* **1989**, *370*, 263−276. − [2f] S. Sakuraba, T. Morimoto, K. Achiwa, *Tetrahedron: Asymmetry* **1991**, *2*, 597−600. − [2g] K. Angermund, W. Baumann, E. Dinjus, R. Fornika, H. Görls, M. Kessler, C. Krüger, W. Leitner, F. Lutz, *Chem. Eur. J.* **1997**, *3*, 755−764. − [2h] G. Zhu, P. Cao, Q. Jiang, X. Zhang, *J. Am. Chem. Soc*. **1997**, *119*, 1799−1800. − [2i] G. Trabesinger, A. Albinati, N. Feiken, R. W. Kunz, P. S. Pregosin, M. Tschoener, *J. Am. Chem. Soc*. **1997**, *119*, 6315−6323.

[3] [3a] W. S. Knowles, B. D. Vineyard, M. J. Sabacky, B. R. Stults in *Fundamental Research in Homogeneous Catalysis* (Ed.: M. Tsutsui), Plenum Press, New York, **1979**, pp. 537−547. − [3b] W. S. Knowles, *Acc. Chem. Res.* **1983**, *16*, 106−112. − [3c] J. D. Oliver, D. P. Riley, *Organometallics* **1983**, *2*, 1032−1038. − [3d] J. M. Brown, P. L. Evans, *Tetrahedron* **1988**, *44*, 4905−4916. − [3e] J. S. Giovannetti, C. M. Kelly, C. R. Landis, *J. Am. Chem. Soc*. **1993**, *115*, 4040−4057. − [3f] H. Brunner, A. Winter, J. Breu, *J. Organomet. Chem.* **1998**, *553*, 285−306.

[4] [4a] H. B. Kagan in *Comprehensive Organometallic Chemistry*, vol. 8 (Eds.: G. Wilkinson, F. G. A. Stone, E. W. Abel), Pergamon Press, Oxford, **1982**, pp. 463−498. − [4b] V. A. Pavlov, E. I. Klabunovskii, Yu. T. Struchkov, A. A. Voloboev, A. I. Yanovsky, *J. Mol. Catal.* **1988**, *44*, 217−243. − [4c] D. Seebach, D. A. Plattner, A. K. Beck, J. M. Wang, D. Hunziker, W. Petter, *Helv. Chim. Acta* **1992**, *75*, 2171−2209. − [4d] D. Seebach, E. Devaquet, A. Ernst, M. Hayakawa, F. N. M. Kühnle, W. B. Schweizer, B. Weber, *Helv. Chim. Acta* **1995**, *78*, 1636−1650. − [4e] N. M. Brunkan, P. S. White, M. R. Gagne, *Angew. Chem.* **1998**, *110*, 1615−1618; *Angew. Chem. Int. Ed.* **1998**, *37*, 1579−1582.

[5] [5a] I. Toth, B. Hanson, *Organometallics* **1993**, *12*, 1506−1513 and references therein. − [5b] K. Burgess, M. J. Ohlmeyer, K. H. Whitmire, *Organometallics* **1992**, *11*, 3588−3600. − [5c] M. Michalik, T. Freier, M. Schwarze, R. Selke, *Magn. Reson. Chem.* **1995**, *33*, 835−840.

[6] G. Balavoine, S. Brunie, H. B. Kagan, *J. Organomet. Chem*. **1980**, *187*, 125−139.

[7] J. M. Brown, P. A. Chaloner, *J. Am. Chem. Soc*. **1978**, *100*, 4307−4308.

[8] [8a] J. M. Brown, P. A. Chaloner, R. Glaser, S. Geresh, *Tetrahedron* **1980**, *36*, 815−825. − [8b] R. Selke M. Ohff, A. Riepe, *Tetrahedron* **1996**, *52*, 15079−15102.

[9] [9a] J. B. Hendrickson, *J. Am. Chem. Soc*. **1961**, *83*, 4537−4547. − [9b] J. B. Hendrickson, *J. Am. Chem. Soc*. **1967**, *89*, 7036−7046. − [9c] D. F. Bocian, H. L. Strauss, *J. Am. Chem. Soc*. **1977**, *99*, 2876−2882.

[10] [10a] G. R. Brubaker, D. W. Jonson, *Coord. Chem. Rev.* **1984**, *53*, 1−36. − [10b] B. P. Hay, *Coord. Chem. Rev.* **1993**, *126*, 177−236.

[11] V. S. Allured, C. M. Kelly, C. R. Landis, *J. Am. Chem. Soc*. **1991**, *113*, 1−12.

[12] [12a] L. H. Bryant, Jr., A. Lachgar, S. C. Jackels, *Inorg. Chem.* **1995**, *34*, 4230−4238. − [12b] I. Kovacs, M. C. Baird, *Organometallics* **1995**, *14*, 4084−4091 and references therein.

[13] J. B. Hendrickson, *J. Am. Chem. Soc*. **1967**, *89*, 7047−7061.

[14] D. Cremer, J. A. Pople, *J. Am. Chem. Soc*. **1975**, *97*, 1354−1358.

[15] D. F. Bocian, H. M. Pickett, T. C. Rounds, H. L. Strauss, *J. Am. Chem. Soc*. **1975**, *97*, 687−695.

[16] Cambridge Structural Database, Version 5.14, October 1997; see: F. H. Allen, O. Kennard, *Chemical Design Automation News* **1993**, *8*, 31−37.

[17] D. Heller, J. Holz, S. Borns, A. Spannenberg, R. Kempe, U. Schmidt, A. Börner, *Tetrahedron: Asymmetry* **1997**, *8*, 213−222.

[18] M. P. Anderson, L. H. Pignolet, *Inorg. Chem.* **1981**, *20*, 4101−4107.

[19] WIN-DYNAMICS 1.0 Release 951220, NMR Dynamic Spectra Simulation and Iteration, Bruker-Fanzen Analytik GmbH and K. Il'yasov, O. Nedopekin, Bremen, Germany.

[20] [20a] J. M. Brown, P. A. Chaloner, *J. Organomet. Chem*. **1981**, *217*, C2-C28. − [20b] E. M. Campi, P. S. Elmes, W. R. Jackson, R. J. Thomson, J. A. Weigold, *J. Organomet. Chem*. **1989**, *371*, 393−395.

[21] [21a] V. Elser, H. Strauss, *Chem. Phys. Lett*. **1983**, *96*, 276−278. − [21b] P. M. Ivanov, E. Osawa, *J. Comp. Chem*. **1984**, *5*, 307−313.

[22] [22a] W. B. Moniz, J. A. Dixon, *J. Am. Chem. Soc*. **1961**, *83*, 1671−1675. − [22b] N. −J. Schneider, N. Nguyen-Ba, *Org. Magn. Reson.* **1982**, *18*, 38−41.

[23] R. Selke, H. Pracejus, *J. Mol. Catal.* **1986**, *37*, 213−225.

[24] J. Holz, A. Börner, A. Kless, S. Borns, S. Trinkhaus, R. Selke, D. Heller, *Tetrahedron: Asymmetry* **1995**, *8*, 1973−1988.

[25] Available as PCMODEL 4.0 from Serena Software, Bloomington, USA; see: J. J. Gajewski, K. E. Gilbert, J. McKelvy, *Adv. Mol. Model*. **1990**, *2*, 65.

[26] B. P. Hay, J. R. Rustad, *J. Am. Chem. Soc*. **1994**, *116*, 6316−6326 and references therein.

[27] M. J. Frisch, G. W. Trucks, H. B. Schlegel, P. M. W. Gill, B. G. Johnson, M. A. Robb, J. R. Cheeseman, T. Keith, G. A. Petersson, J. A. Montgomery, K. Raghavachari, M. A. Al-Laham, V. G. Zakrzewski, J. V. Ortiz, J. B. Foresman, J. Cioslowski, B. B. Stefanov, A. Nanayakkara, M. Challacombe, C. Y. Peng, P. Y. Ayala, W. Chen, M. W. Wong, J. L. Andres, E. S. Replogle, R. Gomperts, R. L. Martin, D. J. Fox, J. S. Binkley, D. J. Defrees, J. Baker, J. P. Stewart, M. Head-Gordon, C. Gonzalez, and J. A. Pople, *Gaussian 94, Revision E.2*, Gaussian, Inc., Pittsburgh PA, **1995**.

[28] K. Tamao, K. Nakamura, S. Yamaguchi, M. Shiro, S. Saito, *Chem. Lett.* **1996**, 1007−1008.

Received August 4, 1998
[I98262]